REVIEWS in MINERALOGY and GEOCHEMISTRY

Volume 41 2000

HIGH-TEMPERATURE AND HIGH-PRESSURE CRYSTAL CHEMISTRY

Editors:

ROBERT M. HAZEN

Geophysical Laboratory
Center for High-Pressure Research
Carnegie Institution of Washington
Washington, DC

ROBERT T. DOWNS

Department of Geosciences
University of Arizona
Tucson, Arizona

COVER: A polyhedral representation of the crystal structure of quartz, SiO_2, as it changes with pressure and with temperature. The pressure change is from 26 GPa to 0 GPa, extrapolated from Glinnemann et al (1992). The temperature change is from room temperature to 848 K, through the α-β transition, using data from Kihara (1990). See Chapter 4, page 89ff for details on producing the animation.

Series Editor: ***Paul H. Ribbe***
Virginia Polytechnic Institute and State University
Blacksburg, Virginia

MINERALOGICAL SOCIETY of AMERICA

2

Equations of State

R. J. Angel*

Bayerisches Geoinstitut
Universität Bayreuth
D95440 Bayreuth, Germany

*Present address: *Department of Geological Sciences, Virginia Tech, Blacksburg, VA 24061*

INTRODUCTION

Diffraction experiments at high pressures provide measurement of the variation of the unit-cell parameters of the sample with pressure and thereby the variation of its volume (or equivalently its density) with pressure, and sometimes temperature. This last is known as the 'Equation of State' (EoS) of the material. It is the aim of this chapter to present a detailed guide to the methods by which the parameters of EoS can be obtained from experimental compression data, and the diagnostic tools by which the quality of the results can be assessed. The chapter concludes with a presentation of a method by which the uncertainties in EoS parameters can be predicted from the uncertainties in the measurements of pressure and temperature, thus allowing high-pressure diffraction experiments to be designed in advance to yield the required precision in results.

The variation of the volume of a solid with pressure is characterised by the bulk modulus, defined as $K = -V\partial P/\partial V$. Measured equations of state are usually parameterized in terms of the values of the bulk modulus and its pressure derivatives, $K' = \partial K/\partial P$ and $K'' = \partial^2 K/\partial P^2$, evaluated at zero pressure. These zero-pressure (or, almost equivalent, the room-pressure values) are normally denoted by a subscript "0," thus: $K_0 = -V_0(\partial P/\partial V)_{P=0}$, $K_0' = (\partial K/\partial P)_{P=0}$, and $K_0'' = (\partial^2 K/\partial P^2)_{P=0}$. However, throughout this chapter a number of notational conventions are followed for ease of presentation. Unless specifically stated, the symbols K' and K'' (without subscript) refer to the zero-pressure values at ambient temperature, all references to bulk modulus, K_0, and its derivatives K', K'' and $\partial K_0/\partial T$ refer to isothermal values and all compression values, $\eta = V/V_0$, and variables such as finite strain f derived from them, are similarly isothermal quantities. The relationship between the isothermal bulk modulus, more generally denoted K_T, and the adiabatic bulk modulus K_S that describes compression in a thermally closed system (at constant entropy) is $K_s = K_T(1+\alpha\gamma T)$ where α is the volume thermal expansion coefficient and γ is the Gruneisen parameter.

EOS FORMULATIONS

The derivation of EoS for solids is dealt with in detail in a number of recent texts (e.g. Anderson 1995, Duffy and Wang 1998), and will not be repeated here. It is sufficient to note that there is no absolute thermodynamic basis for specifying the correct form of the EoS of solids. Therefore, all EoS that have been developed and are in widespread use are based upon a number of assumptions. The validity of such assumptions can only be judged in terms of whether the derived EoS reproduces experimental data for volume or elasticity. Of the many developed EoS (see Anderson 1995) only the ones commonly used to fit *P-V* and *P-V-T* data are presented here. The further constraints on EoS, such as αK_{0T} = constant, that can be applied at temperatures in excess of the Debye temperature (e.g. Anderson 1995) are not considered here because most experimental datasets include

1529-6466/00/0041-0002$05.00

data from lower temperatures.

Isothermal EoS

Murnaghan. The Murnaghan EoS (Murnaghan 1937) can be derived from the assumption that the bulk modulus varies linearly with pressure, which results in a relationship between P and V of:

$$V = V_0\left(1+\frac{K'P}{K_0}\right)^{-1/K'} \tag{1}$$

or as:

$$P = \frac{K_0}{K'}\left[\left(\frac{V_0}{V}\right)^{K'} - 1\right] \tag{2}$$

It is found experimentally that this EoS reproduces both P-V data and the correct values of the room pressure bulk modulus for compressions up to about 10% (i.e. $\eta = V/V_0 > 0.9$, Fig. 1). The simple functional form of this EoS that allows algebraic solution of P in terms of V and vice-versa has led to its widespread incorporation into thermodynamic databases used for calculating metamorphic phase equilibria (e.g. Holland and Powell 1998, Chatterjee et al. 1998). Note that the frequent choice of fixing $K' = 4$ (e.g. Holland and Powell 1998) to obtain a two-parameter Murnaghan EoS in terms of just V_0 and K_0 has no basis in its derivation. On the contrary, $K' = 4$ is obtained from truncation of the Birch-Murnaghan finite strain EoS to second order.

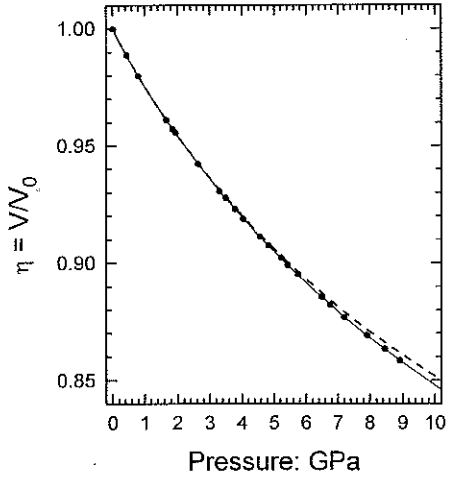

Figure 1. Volume-pressure data for quartz. The solid line is a fit of the Birch-Murnaghan 3rd order EoS (with parameters given in Table 1) to the data points from Angel et al. (1997). The compression predicted by a Murnaghan EoS with the same values of K_0 and K' (dashed line) deviates significantly from the observed data for $\eta < 0.90$. This demonstrates that values of K_0 and K' are not transferable between these two EoS. The Murnaghan EoS fitted to the data (Table 1) is indistinguishable in this plot from the Birch-Murnaghan 3rd order EoS.

Birch-Murnaghan. Finite strain EoS are based upon the assumption (e.g. Birch 1947) that the strain energy of a solid undergoing compression can be expressed as a Taylor series in the finite strain, f. There are a number of alternative definitions of f, each of which leads to a different relationship between P and V. The Birch-Murnaghan EoS (Birch 1947) is based upon the Eulerian strain, $f_E = \left[\left(V_0/V\right)^{2/3} - 1\right]/2$. Expansion to fourth order in the strain yields an EoS:

$$P = 3K_0 f_E\left(1+2f_E\right)^{5/2}\left(1+\frac{3}{2}(K'-4)f_E + \frac{3}{2}\left(K_0K'' + (K'-4)(K'-3) + \frac{35}{9}\right)f_E^2\right) \tag{3}$$

If this EoS is truncated at second order in the energy, then the coefficient of f_E must be identical to zero, which requires that K' has the fixed value of 4 (higher-order terms are ignored).The 3rd-order truncation, in which the coefficient of f_E^2 is set to zero yields a three-parameter EoS (with V_0, K_0 and K') with an implied value of K'' given by (Anderson 1995):

$$K'' = \frac{-1}{K_0}\left((3-K')(4-K')+\frac{35}{9}\right) \tag{4}$$

Natural strain. Poirier and Tarantola (1998) developed an EoS based upon the "natural" or "Hencky" measure of linear strain, $f_N = \ln(l/l_0)$ which, for hydrostatic compression, may be written as $f_N = 1/3\ln(V/V_0)$. This yields a pressure-volume relationship expanded to fourth order in strain of:

$$P = 3K_0\left(\frac{V_0}{V}\right)f_N\left[1+\frac{3}{2}(K'-2)f_N+\frac{3}{2}\left(1+K_0K''+(K'-2)+(K'-2)^2\right)f_N^2\right] \tag{5}$$

Examination of Equation (5) shows that truncation of this "Natural strain" EoS at second order in the strain implies a value of $K' = 2$, different from that of the 2nd-order Birch-Murnaghan EoS. For truncation at third order in the strain, the implied value of K'' is given by:

$$K'' = \frac{-1}{K_0}\left[1+(K'-2)+(K'-2)^2\right] \tag{6}$$

This value for K'' is normally substantially larger than that implied by the truncation of the 3rd-order Birch-Murnaghan EoS (Eqn. 4), and this may result in significantly different values of K_0 being obtained from fits of the two equations to the same P-V data.

Vinet. The finite-strain EoS do not accurately represent the volume variation of most solids under very high compression ($\eta < 0.6$), so Vinet et al. (1986, 1987a) derived an EoS from a general inter-atomic potential. For simple solids under very high compressions the resulting Vinet EoS provides a more accurate representation of the volume variation with pressure:

$$P = 3K_0\frac{(1-f_V)}{f_V^2}\exp\left(\frac{3}{2}(K'-1)(1-f_V)\right) \tag{7}$$

where $f_V = (V/V_0)^{1/3}$. There is no theoretical basis for truncation of the EoS to lower order, although examination of Equation (7) shows that such truncation yields an implied value for K' of 1. The value of K'' implied by Equation (7) is given by Jeanloz (1988) as:

$$K'' = \frac{-1}{K_0}\left[\left(\frac{K'}{2}\right)^2+\left(\frac{K'}{2}\right)-\left(\frac{19}{36}\right)\right] \tag{8}$$

Expansions of the Vinet EoS to include a refineable K'' have been proposed but are not required to fit most experimental P-V and P-V-T data of simple solids. Despite being often called a "Universal EoS" (e.g. Vinet et al. 1986, 1987a) it should be noted that the Vinet EoS is not intended for materials with significant degrees of internal structural freedom such as bond-bending (Jeanloz 1988).

Thermal equations of state

From an experimental viewpoint, the simplest method for evaluating P-V-T data is to use an isothermal EoS, such as those given above, and to consider the parameters V_0 and K_0 as being the material properties at P = 0 but at elevated temperature T. The high-

temperature value of the zero-pressure volume is:

$$V_0(T) = V_0(T_0)\exp\int_{T_0}^{T}\alpha(T)dT \tag{9}$$

which is derived by integration of the thermodynamic definition of the thermal expansion coefficient $\alpha(T) = V^{-1}\partial V/\partial T$. As for the compression of solids, there is no general thermodynamic theory that specifies the form of the function $\alpha(T)$, e.g. Krishnan et al. (1979). At the lowest level of approximation $\alpha(T)$ can be considered a constant, or to vary with linearly with temperature as $\alpha(T) = a + bT$, but higher-order terms can be employed when necessary (e.g. Saxena and Zhang 1990). A summary of frequently-used formulations is provided by Fei (1995).

Within the uncertainties of most current experimental measurements, the variation of bulk modulus with temperature can be considered to be linear:

$$K_0(T) = K_0(T_0) + (T - T_0)\left(\frac{\partial K}{\partial T}\right)_P \tag{10}$$

in which T_0 is a reference temperature (usually 298 K). This formulation, combined with use of a variable K' in the associated isothermal EoS, includes all second derivatives of the volume with respect to the intensive variables P and T, and is usually sufficient to fit most experimental P-V-T datasets collected from room temperature up to ~1000 K. The derivations of thermal EoS more applicable to higher-temperature datasets are given by Duffy and Wang (1998). A simplified extension of the Vinet EoS to variable temperature developed by Vinet et al. (1987b) is only applicable above the Debye temperature.

Cell parameter variation

While many experimental P-V data sets are fitted with one of the isothermal EoS described above, it is not unusual to find the cell parameter variation with pressure fitted with a polynomial expression such as $a = a_0 + a_1P + a_2P^2$, or even with a simple linear relationship. While such an expression may indeed describe low-precision data adequately within the error bars, it is both unphysical and inconsistent with use of an EoS for the P-V data. A linear expression implies that the material does not become stiffer under pressure, while a quadratic form will have a negative coefficient for P^2, implying that at sufficiently high pressures the material will expand with increasing pressure. A consistent alternative is provided by linearization of any of the isothermal EoS described above through the substitution of the cube of a lattice parameter for the volume in the equations. The value of "*linear*-K_0" obtained from fitting the isothermal equation is then one-third of the inverse of the zero-pressure linear compressibility β_0 of the axis, defined as $\beta_0 = l_0^{-1}(\partial l/\partial P)_{P=0}$ in which l_0 is the length of the unit-cell axis at zero pressure.

In the general case, the stress applied to a crystal is a second-rank tensor, denoted σ. The application of such a stress gives rise to different changes in length, and thus different strains, in different directions of the crystal (unless it is cubic). If the strains remain linearly dependent upon the applied stress (i.e. in the Hooke's law regime) then they also comprise a second-rank tensor, denoted ε. The general relationship between the stress and the strain is given by the tensor equation $\varepsilon_{ij} = s_{ijkl}\sigma_{kl}$ (e.g. Nye 1957) in which s is the elastic compliance tensor (elastic modulus tensor in English). In the case of hydrostatic compression there are no shear stresses and thus the off-diagonal components of the stress tensor are zero, while the diagonal terms are equal to the applied pressure; $\sigma_{kl} = -P$ for $k=l$ and $\sigma_{kl} = 0$ for $k \neq l$. The stress-strain relationship for hydrostatic compression therefore becomes $\varepsilon_{ij} = -Ps_{ijkk}$. The fractional volume change of the crystal under stress is given by the sum of the diagonal terms of the strain tensor, thus $\Delta V/V = \varepsilon_{ii} = -Ps_{iikk}$, from which it

follows that the isothermal volume compressibility is s_{iikk}. If the individual terms of the compliance tensor are written out in matrix notation, the relationship between the *isothermal* elastic compliances of the crystal and the isothermal bulk modulus is obtained: $K = (s_{11}+s_{22}+s_{33}+2s_{12}+2s_{13}+2s_{23})^{-1}$. This relationship is true for all crystal systems.

The linear compressibility, β_l, in any direction in a crystal defined by its direction cosines l_i is $\beta_l = s_{ijkk} l_i l_j$ from which the relationships between the linear compressibilities of the axes and the individual elastic compliances can be obtained (see Nye 1957 for details). For crystals with higher than monoclinic symmetry the definition of the axial compressibilities fully describes the evolution of the unit-cell with pressure. The same is true for temperature and thermal expansion. But for monoclinic crystals one unit-cell angle may change, and in triclinic crystals all three unit-cell angles may change. The full description of the change in unit-cell shape in these cases must therefore include the full definition of the strain tensor resulting from compression and its visualisation as a strain ellipsoid (Nye 1957). A computer program, originally written by Ohashi (1972) is available (see Appendix) to calculate the components and principal axes of strain tensors. The calculation method of Ohashi (1972), further developed by Schlenker et al. (1975) and Jessen and Küppers (1991), is explicitly based upon a finite difference approach. The strain is evaluated from the change in lattice parameters between one data point and the next. Thus the resulting strain tensor represents an average strain over this interval in pressure or temperature. This is a sound approach for crystals of orthorhombic symmetry, or higher, because the orientation of the strain ellipsoid is fixed by symmetry. But for triclinic and monoclinic crystals the strain ellipsoid may rotate with changing P or T. The finite difference calculation of strain then represents an average not only of the magnitudes of the principal axes of the strain ellipsoid, but also an average of their orientation over the finite interval in P or T. An alternative approach which avoids this problem and employs the calculation of the continuous derivatives of the unit-cell parameters with respect to T (or P) has been developed by Paufler and Weber (1999).

FITTING EQUATIONS OF STATE

Least-squares

When fitting EoS one of the variables has to be chosen as the *dependent* variable. From an experimental point of view, one often views volume as the *dependent* variable that results from the choice of a value of the *independent* variables pressure and temperature. On this basis one would expect to fit volume to pressure and temperature in order to determine the parameters of an EoS. However, it is often the case that experimental uncertainties in pressure are greater than, or at least comparable in magnitude with, the uncertainties in compression η, while uncertainties in temperature are much smaller. The choice between pressure and compression as dependent variable is therefore not immediately clear. However, all of the equations of state described in the previous sections can be written in terms of pressure being a function of compression and temperature, $P = f(\eta, T)$, whereas their formulation in the form $\eta = f'(P,T)$ is not usually straightforward. For this reason it is normal to fit EoS in the form $P = f(\eta, T)$ or $P = f(V,T)$.

If the experimental uncertainties in the data set are uncorrelated and normally distributed, the best estimate of the EoS parameters (e.g. V_0, K_0 etc.) can be obtained by the method of "least-squares." The presentation of the details of the implementation of the least-squares method is not appropriate here. For details the reader is recommended to consult a standard statistics text, or the very clear exposition of theory and methodologies given by Press et al. (1986). The presentation here will be restricted to those aspects

especially relevant to the fitting of EoS data, and the interpretation of the results so obtained.

Strictly speaking, a normal distribution of uncertainties only occurs when a large number of data are considered; "large" meaning that the number of data, n, is large compared to $n^{1/2}$. This is not the case for most compression experiments in which n is of the order of 10-20. Therefore care has to be taken to correctly estimate uncertainties and to exclude outliers in the data-set that would otherwise bias the least-squares refinement. Most high-P and high-P,T data are collected in a serial fashion, so serial correlation of errors between data points becomes systematic error which can only be eliminated by careful design of both experiment and instrument. In practice, it is found that these critical assumptions are not sufficiently violated in fitting EoS to invalidate the use of the least-squares method to fit compression data.

The least-squares solution of the EoS can be formalised as being the set of parameters within the EoS function that minimises the weighted sum of the squares of the differences between the observed and calculated pressures at a given volume:

$$\chi^2_w = \frac{1}{n-m}\sum_i^n w_i\left(P_{obs,i} - EoS\left(V_{obs,i}, T_{obs,i}\right)\right)^2 \qquad (11)$$

where n are the number of data points each of which is assigned a weight w_i, and m is the number of parameters being refined. If the EoS can be expressed as a linear combination of separate functions of V and T, then the minimum value of χ^2_w can be found directly by inversion (e.g. Eqn. 29, below). For non-linear problems, such as the direct refinement of K_0 and K' in most EoS, the minimum value of χ^2_w cannot be obtained directly, but must be approached in an iterative manner. For this, the derivatives of the dependent variable, P, with respect to each of the refined parameters (e.g. $\partial P/\partial V_0, \partial P/\partial K_0, \partial P/\partial K'$) must be calculated in each least-squares cycle. Such derivatives can be calculated either analytically or numerically. In the latter case it is important to remember that their accuracy will determine in part the stability and rate of convergence of the non-linear least-squares process towards the minimum value of χ^2_w.

Assignment of weights. In order for the least-squares refinement of the EoS to yield reasonable estimates for both the EoS parameters and their uncertainties, it is important that the correct weighting scheme is applied to the data points in evaluating Equation (11). In general, $w_i = \sigma_i^{-2}$, so the "correct" weighting scheme is that which reflects the true variance, σ_i^2, of each data point which is comprised of a contribution from the uncertainties in the pressure, temperature and volume measurements. Each of these uncertainties may in turn include contributions estimated from the mis-fit of measured data, an estimate from repeat measurements of the same datum, and an estimate of the long-term stability of the instrument. Thus, an individual measurement of a unit-cell volume by X-ray diffraction will have an uncertainty derived from the fit of the unit-cell parameters to the diffraction data itself. But this may not represent the true uncertainty. For example, it is well known that the uncertainties in cell parameters and thus volumes derived from Rietveld or Le-Bail methods of fitting powder diffraction patterns significantly underestimate the true uncertainties (e.g. Young 1993). Improved estimates of the uncertainties can always be obtained by duplicate measurements of the diffraction pattern. Contributions from longer term instrumental instabilities should be determined over the time-scale of the experiment by duplicate measurements of a standard material combined with measurement of the sample at room conditions in the high-pressure apparatus both before and after the high-pressure experiment. These additional uncertainties can often be reduced to a scaling factor for the variance obtained from an individual measurement (e.g. Prince and Spiegelman 1992b). Thus, the estimate of σ^2 obtained from an individual measurement may generally

be replaced by $k\sigma^2$, where k is some empirically determined constant for a given experimental configuration.

If the EoS parameters are to be determined through the minimisation of χ^2_w (Eqn. 11) then the experimental uncertainties in pressure, volume and temperature of a datum must be combined in to a single estimate of the uncertainty of the datum, expressed in terms of the dependent variable, pressure. If the uncertainties in pressure, volume and temperature of a given datum are independent then the combined effective uncertainty in the pressure as the dependent parameter can be obtained as:

$$\sigma^2 = \sigma_p^2 + \sigma_V^2 \cdot \left[\left(\frac{\partial P}{\partial V}\right)_T\right]^2 + \sigma_T^2 \left[\left(\frac{\partial P}{\partial T}\right)_V\right]^2 \tag{12}$$

This propagation of uncertainties is known as the "effective variance method" (Orear 1982). It should be noted that there are a number of technical points involved in the derivation of Equation (12) that may affect the estimates of both the values of the parameters and their uncertainties obtained by least-squares. First, it is assumed that the partial derivatives in Equation (12) are constant over the pressure interval corresponding to σ_V and σ_T which is reasonable this pressure interval is small compared to the bulk modulus of the material. Secondly, although the values of σ obtained through Equation (12) are correct, the derivatives are incorrectly calculated at the experimentally observed values of V and T rather than at the values estimated by the least-squares fit of the EoS. This leads to a slight over-estimate of the parameter uncertainties (Lybanon 1984, Reed 1992), although the effect is usually insignificant for a slowly varying function such as an EoS with small experimental uncertainties in the data.

Through the use of thermodynamic identities (e.g. Anderson 1995), Equation (12) reduces to:

$$\sigma^2 = \sigma_p^2 + \sigma_V^2 \cdot \left(\frac{K}{V}\right)^2 + \sigma_T^2 (\alpha K)^2 \tag{13}$$

where α is the volume thermal expansion coefficient and K is the isothermal bulk modulus of the sample at the temperature and the pressure of the measurement. If the parameters K and α are being refined, the refinement program must recalculate the values of σ, and thus the weights applied to each data point, at the beginning of each least-squares cycle.

The significance of each of the terms in Equation (13) that contribute to the overall uncertainty in a data point can be examined in the context of a material with a bulk modulus of ~100 GPa, and a volume thermal expansion coefficient of ~10^{-5} K^{-1}. For laboratory-based single-crystal diffraction experiments at ambient temperature the uncertainties in pressure are of the order of 0.01 GPa, yielding $\sigma_P^2 = 10^{-4}$ Gpa^2. If temperature fluctuations are of the order of 1 K or less, then the last term in Equation (13) is of the order of 10^{-6} GPa^2 and can be safely ignored. In diffraction experiments at simultaneous high pressures and temperatures, the pressure uncertainty might be of the order of 0.03-0.05 GPa, making $\sigma_P^2 \geq 10^{-3}$ Gpa^2, in which case temperature uncertainties of the order of 10 K would still not contribute significantly to the total variance. On the other hand, even a precision of 0.0001 in σ_V/V (i.e. 1 part in 10,000) will also contribute 10^{-4} GPa^2 to the total variance, indicating that contributions from volume uncertainties should always be included. In lower precision measurements the volume uncertainties may even dominate the total uncertainty.

If pressures have been determined through measurement of the volume of an internal diffraction standard (e.g. Miletich et al., this volume) the uncertainties in pressure and

volume may not be independent because the volumes of both sample and standard may be affected in the same way by the same instrumental fluctuations; monochromator movements leading to wavelength changes are a good example of this sort of problem. In such cases the covariances between P, V and T should be added to Equation (12), although these are often difficult to assess. The practical recourse is to omit the covariances, use Equation (12) as it stands, and to treat the results of the least-squares refinement with caution. Diagnostic statistics such as χ^2_w (see below) can be used to test whether the estimated uncertainties remain reasonable over a series of experiments.

The assignment of an uncertainty to a room pressure measurement of the volume of the sample is especially important because this datum is at one extreme of the data-set and therefore exerts a higher leverage or influence (e.g. Prince and Spiegelman 1992a) on the determination of both V_0 and K_0 than data in the middle of the experimental pressure range. In most cases, and certainly in diamond-anvil cell diffraction experiments, the room-pressure volume can be measured by exactly the same methodology as the high-pressure data. The uncertainty in this datum then comprises the experimentally determined uncertainty in the volume, combined with that of the uncertainty in ambient pressure. A reasonable estimate of the latter might be of the order of 10^{-7}-10^{-6} GPa (1 to 10 mbar) in 10^{-4} GPa (1 bar).

Goodness of fit. The weighted chi-squared, χ^2_w, (Eqn. 11) is not only the function minimised by the least-squares procedure, but it also provides a measure of the quality of the fit once the least-squares process has reached convergence. If the uncertainties in the data are normally distributed then a value of $\chi^2_w = 1$ indicates that the uncertainties have been correctly assessed, that the EoS represented by the refined parameters fits the data, and that the refinement has converged. In such a case it is found that the fitted EoS passes through the $\pm1\sigma$ error bars of 68.3% of the data points, 95.4% of the $\pm2\sigma$ error bars, etc. A value of $\chi^2_w < 1.0$ has no statistical significance and does not represent a better fit. It may, however, suggest that the uncertainties of the data have been overestimated. A value of $\chi^2_w > 1.0$ indicates that the fitted EoS does not represent the entire data-set and its uncertainties. This may arise from either the EoS model being incorrect in some way, the uncertainties of the data being underestimated, or a few data points having wrong values. Such outliers can be identified by comparing the misfits of individual data points $|P_{obs}-P_{calc}|$ with their estimated uncertainties. Those data with the largest values of $|P_{obs}-P_{calc}|/\sigma$ are termed "outliers". If there is a sound experimental reason for doing so (e.g. non-hydrostatic pressure conditions), the outliers may be excluded from subsequent fitting of the EoS, in which case χ^2_w will decrease. But, the denominator $n-m$ in the expression for χ^2_w will also decrease, so exclusion of data points that are not outliers may be indicated by a subsequent increase in χ^2_w. Misfit of the EoS may also be due to a parameter being fixed to an inappropriate value when it should be refined; the addition of a parameter to the refinement will always reduce the total misfit to the data. But, because χ^2_w includes the number of degrees of freedom, n-m, of the fit, if the additional parameter does not significantly improve the fit to the data, χ^2_w will increase because $n-m$ will have decreased by 1. A proper statistical assessment of the significance of the addition of a parameter to a refinement is provided by the "F-test" (e.g. Prince and Spiegelman 1992a).

Variances and covariances. At convergence of the least-squares refinement, the variance-covariance matrix, $\mathbf{V}^a$, of the refined parameters can be calculated from the normal-equations matrix used in the non-linear least-squares refinement (e.g. Press et al. 1986, Prince and Boggs 1992). The definition of $\mathbf{V}^a$ for the simpler case of linear-least-squares is given below in Equation (30). The diagonal elements of the variance-covariance matrix, $\mathbf{V}^a_{i,i}$, are estimates of the *variances* of the refined values of the EoS parameters. Thus the *estimated standard deviation* of the i^{th} refined parameter is $\sqrt{\mathbf{V}^a_{i,i}}$, provided that the

refinement is converged and that $\chi^2_w = 1$. If, at convergence $\chi^2_w > 1$ but the model is believed to be correct, then the larger value of χ^2_w is usually attributed to an under-estimate of the uncertainties of the experimental data. Then it is normal practice to multiply all of the elements of the variance-covariance matrix by χ^2_w (e.g. Press et al. 1986, Prince and Spiegelman 1992b). This is equivalent to multiplying the uncertainties of all of the experimental data points by a factor $\sqrt{\chi^2_w}$. A word of caution is necessary here. Many least-squares refinement programs rescale the variance-covariance matrix automatically, and many also do so irrespective of the value of χ^2_w. If $\chi^2_w < 1$ there is no argument (see above) for making the multiplication which, if performed, will make the reported parameter esd's smaller.

The off-diagonal elements of the variance-covariance matrix such as $\mathbf{V}^a_{i,j}$ are the *covariances* of the parameters a_i and a_j. They measure the degree to which the values of two refined variables are correlated. Note that the covariance of two refined parameters has the units of the product of the two parameters themselves; the covariance of, for example, V_0 and K_0, could be in units of $Å^3$ GPa. The absolute value of the covariance therefore depends on the units used for the EoS parameters. A more understandable measure of the degree to which two parameters are inter-dependent is provided by normalising the covariance by the variances of the parameters to obtain a *correlation coefficient*:

$$Corr(i,j) = \frac{\mathbf{V}^a_{i,j}}{\sqrt{\mathbf{V}^a_{i,i}\mathbf{V}^a_{j,j}}} \tag{14}$$

The correlation coefficient always has a value between -1 and +1, although it is often multiplied by 100 and expressed as a percentage. A value of zero indicates that the two parameters are completely uncorrelated, and thus are determined completely independently of one another. If the correlation coefficient is non-zero, then the two parameter values are partially dependent upon one another. A positive value indicates that the data can be fitted almost as well by increasing both parameters simultaneously, a negative value that increasing one parameter and decreasing the other will lead to almost as good a fit. Non-zero values of covariances, and thus correlation coefficients, therefore increase the total uncertainty in the parameter values beyond that derived from the variances of the individual parameters alone. The effect of covariance is best visualised through use of confidence ellipses, whose construction is illustrated by a worked example in a later section of this chapter. In the limit, the correlation coefficient can have values of +1 or -1. Such values indicate that the two parameters are completely correlated, and cannot be determined independently from the data because an infinite number of pairs of values of the parameters provides an equally good fit to the data. In such a case their values cannot be uniquely determined by the least-squares process and, indeed, most least-squares programs will terminate under such circumstances because the least-squares matrix becomes singular and therefore cannot be inverted.

It is not uncommon to fit an EoS in an algebraic form in which the refined parameters a_i are not the parameters such as K_0 and K' that we require, but some combination of them. If we denote this second set of desired parameters b_i, then we will have a set of equations linking them to the a_i through which the least-squares estimates of their values may be obtained directly. The variances and the covariances of the transformed parameters b_i are then given by the components of the matrix $\mathbf{V}^b$ which may obtained from the variance-covariance matrix of the a_i set of parameters through:

$$\mathrm{V}^b_{k,l} = \sum_i \sum_j \mathrm{V}^a_{i,j} \left(\frac{\partial b_k}{\partial a_i}\right)\left(\frac{\partial b_l}{\partial a_j}\right) \tag{15}$$

Note that the existence of this transformation implies that, provided the weights used in the least-squares procedure were also transformed correctly and that an equivalent set of parameters are refined in each case, the same refined parameters and the same esd's will be obtained from a fit of a particular EoS *irrespective* of the way in which the EoS is formulated. The transformation can also be used to calculate the uncertainties in K and K′ at higher pressures, as illustrated below.

Practical considerations

It is important to bear in mind that the formulation of all EoS means that their parameters can be highly correlated, and therefore care has to be taken in choosing which parameters to refine and which to fix. Such decisions influence the final values of the refined parameters, so care must also be taken in their interpretation. In this section a practical guide to addressing these issues in a conservative manner is presented.

Refinement strategy. Examination of the equations of all isothermal EoS (Eqns. 1-8) shows that they are non-dimensional; they can all be written in terms of P/K_0 and V/V_0 Therefore K_0 and V_0 have the same units as the experimental pressures and volumes respectively and are the scaling parameters of an EoS. In particular, V_0 is a quantity that is dependent upon the calibration of the technique used to measure the volumes. For example, in single-crystal diffraction, the algorithms used to determine the Bragg angles of reflections often lead to a strong dependence of unit-cell volume on the Bragg angle (see Angel et al., this volume). In monochromatic angle-dispersive powder diffraction, the volumes obtained from fitting the powder pattern will depend upon the alignment of the monochromator and the value of the resulting X-ray wavelength. Similarly, in energy-dispersive diffraction the volume is dependent upon the energy calibration of the detector. In all of these cases the volumes measured at high pressures may be on a different scale from some high-accuracy value of V_0 determined by another technique. As demonstrated by Hazen and Finger (1989), the fixing of V_0 to such an inappropriate value can lead to incorrect estimates of the other EoS parameters being obtained from the least-squares refinement to high-pressure volume data.

The parameters V_0 and K_0 thus have the largest influence on the calculated pressure and should always be refined. For isothermal data sets the first stage of refinement should therefore be the refinement of V_0 and K_0 alone in a 2nd-order EoS, with the next higher order term, K' set to its implied value. Then K' is refined, along with the previous parameters, and the significance, as measured by the change in χ^2_w, of its addition is assessed. This process is continued until the addition of further parameters yields no significant improvement in the fit of the EoS to the experimental data. If, at any stage, the additional parameter results in a significant improvement in the fit, then the χ^2_w value will decrease, as will the esd's of the parameters refined in the previous stage. And the deviation of the refined value of the parameter from the value implied by the truncation of the EoS to lower order will be larger than the *esd* of the refined parameter. If the additional parameter does not improve the fit to the data, then χ^2_w will increase or stay the same, the esd's of the other parameters will increase (due to their correlation with the additional parameter) and the value of this additional parameter will not deviate significantly from the value implied by the lower-order truncation of the EoS.

A practical demonstration of this process is given in Table 1 which lists the results of step-wise refinements of three EoS to the 23 *P-V* data for quartz reported by Angel et al. (1997). All fits were performed with the program EOSFIT (see Appendix) and with full weights assigned to each data point (Eqn. 13). The first refinement of the Birch-Murnaghan EoS has K' fixed at 4, the value implied by the 2nd-order truncation in strain. The large value of 128 for χ^2_w, together with the maximum misfit, $|P_{obs}-P_{calc}|_{max}$, more than ten times

Table 1. EoS parameters fitted to the quartz *P-V* data of Angel et al. (1997)

	$V_0 : Å^3$	$K_0 : GPa$	K'	$K'' : GPa^{-1}$	χ^2_w	$\lvert P_{obs} - P_{calc} \rvert_{max}\ GPa$
BM2	112.97(2)	41.5(3)	[4.0]	[-.094]	128	0.32
BM3	112.981(2)	37.12(9)	5.99(5)	[-.265]	0.95	0.025
BM4	112.981(2)	36.89(22)	6.26(24)	-0.41(12)	0.93	0.026
NS2	112.95(5)	46.5(6)	[2.0]	[-0.022]	580	0.65
NS3	112.982(2)	36.39(11)	6.91(7)	[-0.825]	1.15	0.026
NS4	112.981(2)	36.90(24)	6.25(29)	-0.39(11)	0.93	0.026
Vinet	112.981(2)	37.02(9)	6.10(4)	[-0.319]	0.90	0.025
Murn.	112.981(2)	37.63(10)	5.43(4)	[0]	1.57	0.033

Note: Numbers in parentheses represent esd's in the last digit. Numbers in square brackets are the implied values of the parameters.

larger than the esd in an individual data point indicates that this EoS does not represent the data. Expansion of the EoS to third order reduces χ^2_w to 0.95, indicating a significant improvement to the fit. The same conclusion would be drawn from the other indicators; the refined value of the additional parameter K' (5.99) differs by 50 esd's from the previously implied value of $K' = 4$, the esd's of V_0 and K_0 have decreased, the maximum misfit is similar to the estimates of the uncertainties in pressure estimated directly from the experiment, and the value of V_0 is identical to that determined experimentally. Further expansion of the EoS to fourth order, including refinement of K'', yields only a marginal improvement in χ^2_w, because the refined value only differs marginally significantly (1.2 esd's) from the value implied by the 3rd-order truncation of the EoS. Note also that the esd's of K_0 and K' have increased significantly in this last refinement due to their strong correlation (93.6% and -99.2% respectively) with K''. For practical purposes, therefore, the 3rd-order Birch-Murnaghan EoS would be considered to yield an adequate representation of the data-set.

The steps in the refinement of the Natural Strain EoS to the same data-set (Table 1) are similar, except for the choice of termination of the refinement process. In this case further expansion of the Natural Strain EoS to 4th order results in a significant decrease in χ^2_w from 1.15 to 0.93 as a result of the value of K'' deviating by more than 4 esd's from the value implied by the 3rd-order truncation (Eqn. 6).

When *P-V-T* data are fitted, a procedure equivalent to the isothermal case should be followed, except that the parameter set is expanded to include temperature-dependent terms such as the thermal expansion and the temperature variation of the bulk modulus. In order to avoid biasing other parameters it is important to refine together all of the EoS parameters which can be expressed as the same order of derivative of volume with respect to pressure and temperature (Plymate and Stout 1989). Thus, the first stage of refinement should involve V_0, together with the 1st-order derivatives K_0 and a temperature-independent thermal expansion coefficient α. The next set of parameters to add are the 2nd-order volume derivatives, K', dK/dT and $d\alpha/dT$, each expressed as a constant. The values should only be set to zero (or implied value for K') and not refined if refinement results in values that do not significantly improve the fit to the data.

Additional care must be taken in fitting a *P-V-T* EoS when data from different types of experiments are combined together, for example single-crystal compression measurements made at room temperature with simultaneous high-temperature, high-pressure powder diffraction measurements. Then it is important to ensure that both the volumes and the pressures from the two or more methods are on the same scale; the former is easily obtained by dividing each separate set of volumes by the value obtained by each method at ambient conditions. The question of pressure scales is more difficult, but is ideally addressed by using the same material as an internal diffraction standard in all of the experiments. It is also important to ensure that the relative weighting of the datasets is correct, by employing Equation (13) to propagate realistic assessments of the uncertainties of all experiments. In doing so, it is normal to find that the room-temperature compression data and the room-pressure thermal expansion data are weighted much more heavily than the simultaneous high-P,T data. Failure to assign weights can lead to significantly different values for the EoS parameters, as illustrated by Zhao et al. (1995).

The f-F plot. The precision with which volumes and pressures can now be measured means that it is very difficult to obtain a useful visual assessment of the quality of a EoS fit from a direct plot of volume against pressure. Nor do *P-V* plots such as Figure 1 provide a visual indication of which higher order terms such as K' and K'' might be significant in an EoS. Such a visual diagnostic tool is provided by the *F-f* plot, which can be applied to any isothermal EoS based upon finite strain. For the Birch-Murnaghan EoS, based upon the Eulerian definition of finite strain f_E, a "normalised stress" is defined as $F_E = P/3f_E(1+2f_E)^{5/2}$, and the EoS (Eqn. 3) can be re-written as a polynomial in the strain (e.g. Stacey et al. 1981):

$$F_E = K_0 + \frac{3K_0}{2}\left(K_0' - 4\right)f_E + \frac{3K_0}{2}\left(K_0K'' + \left(K' - 4\right)\left(K' - 3\right) + \frac{35}{9}\right)f_E^2 + \ldots \qquad (16)$$

If the P,V data are transformed into f_E and F_E and plotted with f_E as the abscissa a direct indication of the compressional behaviour is obtained. If the data points all lie on a horizontal line of constant F then $K' = 4$, and the data can be fitted with a 2nd-order truncation of the Birch-Murnaghan EoS. If the data lie on an inclined straight line, the slope is equal to $3K_0(K'-4)/2$, and the data will be adequately described by a 3rd-order truncation of the EoS, as is the case for the quartz data plotted in Figure 2. In a few rare cases it is found that the value of K'' differs significantly from the value implied by the 3rd-order truncation, in which case the coefficient of f^2 in Equation (16) is not zero, and the data fall on a parabolic curve in the *F-f* plot (Fig. 2). In all cases, the intercept on the F axis is the value of K_0.

For proper assessment of an *f-F* plot, the uncertainties in f_E and F_E must also be considered. These may be calculated by propagation of the experimental uncertainties in compression, $\eta = V/V_0$, and pressure (Heinz and Jeanloz 1984):

$$\sigma_f = \frac{1}{3}\eta^{-5/3}\sigma_\eta \qquad (17)$$

$$\sigma_F = F_E\sqrt{\left(\sigma_P/P\right)^2 + \left(\sigma'\right)^2} \qquad (18)$$

where $\sigma' = \left(7\eta^{-2/3} - 5\right)\sigma_\eta/3\left(1-\eta^{-2/3}\right)\eta$ is the estimated fractional uncertainty in $f_E\left(1+2f_E\right)^{5/2}$. Note that these expressions are in a different form from, but equivalent to, those in Heinz and Jeanloz (1984). Both this uncertainty and the fractional uncertainty σ_P/P will decrease with increasing pressure if the absolute measurement uncertainties in pressure and volume remain constant, resulting in the decrease in σ_F typically observed (e.g. Fig. 2). The relative magnitudes of the experimental uncertainties in pressure and volume obviously

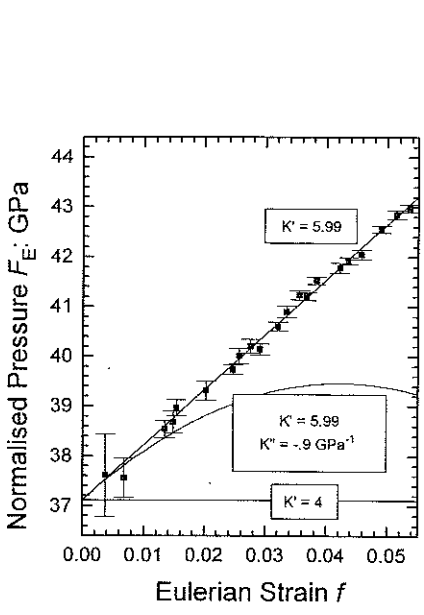

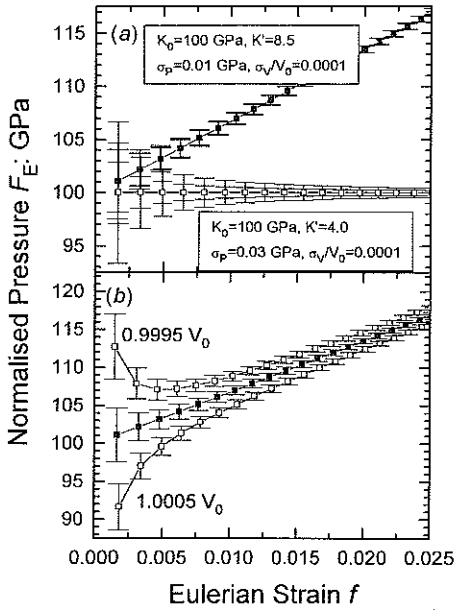

Figure 2 (left). An *F-f* plot based on the Birch-Murnaghan EoS. The data points are the quartz data plotted in Figure 1, with error bars calculated through Equation (18). The plots of F_E with f_E for other values of K' and K'' are also shown to illustrate that the plot yields an immediate indication of the order of the EoS necessary to fit the data.

Figure 3 (right). (a) The relative contributions of uncertainties in P and V to the uncertainty in F. For $\sigma_V = 10^{-4}V_0$, and $\sigma_P = 0.03$ GPa the contributions are approximately equal, whereas for $\sigma_P = 0.01$ GPa the uncertainty in volume (inner error bars) dominates. (b) The use of an incorrect value for V_0 results in abnormal curvature on the *F-f* plot (two datasets with open symbols) compared to the correctly calculated data (filled symbols). Note that the effect is especially severe at small values of compression (i.e. small f).

determine which contributes most to σ_F. Figure 3a shows two synthetic datasets in which $\sigma_V = 10^{-4}V_0$, and $\sigma_P = 0.01$ GPa and 0.03 GPa respectively. For the smaller uncertainty in pressure the uncertainty in F is dominated by σ_V, whereas for the larger σ_P the pressure and volume uncertainties contribute about equally. In both cases σ_F is of the order of $0.01F$ even at high pressures, whereas Equation (17) shows that the uncertainty in f_E is of the order of σ_η. Thus σ_f will typically be of the order of 10^{-3} to $10^{-4}f_E$ and is therefore usually ignored.

The equivalent expressions for the Natural Strain EoS are $F_N = PV/3f_N V_0 = P\eta/\ln\eta$ and

$$\sigma_f = \frac{1}{3}\eta^{-1}\sigma_\eta \tag{19}$$

$$\sigma_F = F_N\sqrt{(\sigma_P/P)^2 + (\sigma')^2} \tag{20}$$

where $\sigma' = \left(1-(\ln\eta)^{-1}\right)\sigma_\eta/\eta$ is the estimated fractional uncertainty in the quantity $\eta/\ln\eta$. From these an analysis equivalent to that for the Birch-Murnaghan equation can be made by reference to Equation (5).

For the Vinet EoS (Eqn. 7) the appropriate plot is of $F_v = \ln\left(Pf_v/3(1-f_v)\right)$ as the

ordinate against $(1-f_v)$ as the abscissa (Vinet et al. 1986, 1987a; Schlosser and Ferrante 1988), which should yield a straight line with an intercept of $\ln(K_0)$ and a slope of $3(K'-1)/2$. The uncertainty in $(1-f_v)$ is simply $\eta^{-2/3}\sigma_\eta/3$ and $\sigma_F = F\sqrt{(\sigma_P/P)^2 + \left(\sigma_\eta/3(\eta^{2/3}-1)\right)^2}$.

It is important to note that for any of these EoS the calculation of both F and f requires *a-priori* knowledge of the value of V_0. Thus, while these plots provide a good visual estimate of the order of the EoS and the parameter values, they cannot be used to determine V_0. Therefore the plots and the *f-F* formalism should not be used to obtain values of the other EoS parameters by refinement. Note also that use of an incorrect value of V_0 produces an anomalous curvature in the *f-F* plot (Fig. 3b). Such curvature is easily mistaken as indicating a value of K'' that deviates significantly from the value implied by a 3rd-order truncation of the EoS. This is also a graphical display of the phenomenon discussed above and by Hazen and Finger (1989); all other EoS parameters will be biased if V_0 is fixed to an inappropriate value.

For non-quenchable high-pressure phases V_0 cannot be measured and thus f and F cannot be calculated from the data. Following earlier iterative approaches to obtaining an *f-F* plot of such data, Jeanloz (1981) provided an analytic method of renormalizing the data which allows not only a plot analogous to the *f-F* plot to be derived but also proper estimates of the parameter uncertainties to be obtained. For *P-V-T* data there are two ways in which an *f-F* plot can be obtained. If the data were collected as a set of isothermal series, then each series can be separately analysed using V_0(T) to obtain separate *f-F* plots. An alternative approach, applicable to all *P-V-T* data-sets, would be to use the thermal expansion coefficient to reduce all of the data to a common temperature and to construct a single *f-F* plot.

Confidence ellipses. It is quite normal in fitting EoS to compression data to find that the correlation coefficient (Eqn. 14) between K_0 and K' is of the order of -0.90 to -0.95 (i.e. -90 to -95%), indicating that the data can be fitted almost equally well by decreasing the value of K_0 and increasing the value of K', or vice-versa. Such strong correlation must be considered when comparing a set of EoS parameters determined by least-squares with independently determined values of K_0 and K'. The extent of this correlation is best visualised by constructing a series of *confidence ellipses* in the parameter space whose axes x and y represent values of K_0 and K' (Bass et al. 1981). The first step in calculating a confidence ellipse is to construct a 2x2 square matrix which consists of the variances and covariance of K_0 and K' obtained from the least-squares procedure. Then the equation of a confidence ellipse is given by the matrix equation:

$$\Delta = (x,y)\begin{pmatrix} V_{K,K} & V_{K,K'} \\ V_{K,K'} & V_{K'K'} \end{pmatrix}^{-1}\begin{pmatrix} x \\ y \end{pmatrix} \qquad (21)$$

where Δ is a value from the chi-square distribution with 2 degrees of freedom, chosen for the level of confidence required. Thus Δ = 2.30 for a 68.3% confidence level (i.e. the equivalent of 1σ for a normal distribution of a single variable), Δ = 4.61 for a 90% confidence level, Δ = 6.17 for 95.4% confidence level (2σ) and Δ = 11.8 for 99.73% confidence level (3σ).

If we denote the inverse of the square matrix as $\boldsymbol{U}$, and note that it is symmetric so that its components u_{12} and u_{21} are equal, then Equation (21) can be written in quadratic form as:

$$u_{11}x^2 + 2u_{12}xy + u_{22}y^2 - \Delta = 0 \qquad (22)$$

This equation can be solved for x and y to yield a set of points on an ellipse centred on the origin of the x-y space. These coordinates must then be displaced so that the ellipse is centred on the refined values of K_0 and K'.

As an example of the calculation we take the refinement of the 3rd-order Birch-Murnaghan EoS to the quartz data-set (Table 1). The refined values of K_0 and K' are 37.12 GPa and 5.99 respectively, and the variances are $V_{K,K} = 0.00829$ and $V_{K',K'} = 0.00205$. The covariance from the least-squares fit is $V_{K',K}$ = -.00399. Substituting these values into Equation (21) yields:

$$\Delta = (x,y)\begin{pmatrix} 0.00829 & -.00399 \\ -.00399 & 0.00205 \end{pmatrix}^{-1}\begin{pmatrix} x \\ y \end{pmatrix} = (x \quad y)\begin{pmatrix} 1908 & 3714 \\ 3714 & 7716 \end{pmatrix}\begin{pmatrix} x \\ y \end{pmatrix} \tag{23}$$

Equation (22) for the 68.3% confidence ellipse in K_0 and K' then becomes:

$$1908(x-37.12)^2 + 7428(x-37.12)(y-5.99) + 7716(y-5.99)^2 - 2.30 = 0 \tag{24}$$

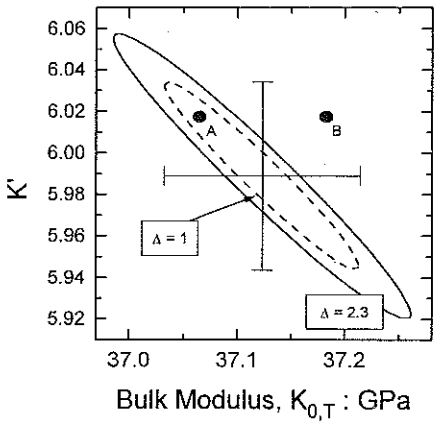

Figure 4. Confidence ellipses in K_0 and K' for the fit of the 3rd-order Birch-Murnaghan EoS to the quartz P-V data (Table 1). Note that the limits of the 1σ error bars obtained from the variances of the two parameters correspond to the limits of a confidence ellipse calculated with Δ = 1 (dashed line), *not* to the ellipse calculated for two degrees of freedom (with Δ = 2.30).

This ellipse is drawn as the solid line in Figure 4. It is strongly elongated with negative slope, reflecting the strong negative correlation of the parameters K_0 and K'. The ellipse encloses an area in the K_0 – K' parameter space within which there is a 68.3% chance that the true values of K_0 and K' lie. This ellipse is therefore the 2-parameter analogue of a 1σ error bar for a single parameter. Also drawn on Figure 4 are the individual error bars for K_0 and K' obtained from the variances of these parameters. Note that these are *smaller* than the total range of K_0 and K' indicated by the 68.3% confidence ellipse for the two parameters together. Therefore the *esd*'s alone do not represent the true uncertainty in the values of K_0 and K'. In fact, they correspond to the limiting values of an ellipse calculated with Δ = 1 (dashed line in Fig. 4), the value corresponding to a 68.3% confidence level from a chi-square distribution with 1 degree of freedom (see, e.g. Press et al. 1986). The limits of the error bars for a single parameter therefore define the range of that parameter within which there would be a 68.3% chance of the true value being found, *independent* of the value of the other parameter.

Other ellipses can be calculated in an analogous manner with the appropriate values of Δ (Fig. 5). These provide a visual confirmation of the conclusions drawn from examining the parameters of the 3rd- and 4th-order fits of the Birch-Murnaghan EoS reported in Table 1. First, the confidence ellipses of the 4th-order fit are significantly larger than those of the 3rd-order fit. Secondly, the point representing the refined parameter values for the

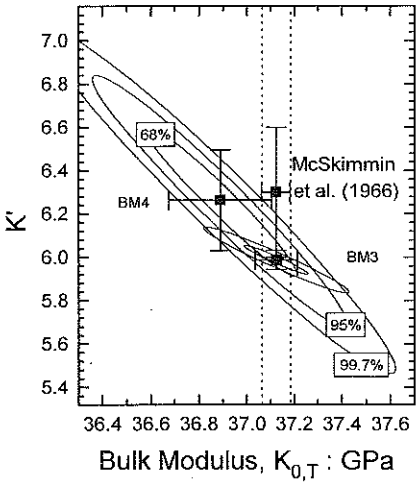

Figure 5. Confidence ellipses for K_0 and K' obtained from the least-squares fit of the quartz *P-V* data. The inner ellipse for the 3rd-order Birch-Murnaghan EoS is that given in Equation (24), the outer is the 99.7% confidence level. The ultrasonic determination of K_0 and K' (McSkimmin et al. 1965) is also shown.

3rd-order EoS lies within the 68.3% (1σ) ellipse for the 4th-order fit, indicating that the addition of the K'' term does not significantly change the parameter values and hence the quality of the fit. If desired, similar plots can be constructed for any pair of refined parameters, such as K' and K'' or α and K_0 etc.

Assessing parameter values. As for any experimental measurements, the values of the refined EoS parameters must be examined for "reasonableness", for which a number of criteria may be employed. First, the esd's of the refined parameters should be approximately those predicted from the known experimental parameters by the method of Bass et al. (1981) which is expanded upon below. Secondly, the refined value of V_0 should be within 1 esd or so of the measured V_0. Significant deviations are usually an indication of an incorrect value for at least one of the other parameters, or a systematic offset between the volumes measured at high pressure and the ambient pressure measurement. In addition, for simple solids in which the compression is controlled by central forces between atoms (e.g. the NaCl structure), it can be shown that the value of K' must lie between 3.8 and 8 (Hofmeister 1993). But this constraint is not applicable to more complex structures such as those whose compression behaviour is dominated by polyhedral tilting (e.g. Yang and Prewitt this volume, Ross this volume).

The *accuracy* of the refined parameters must be assessed by comparison with other measurements of the same quantity. For example the K_0 value can be compared with values obtained from direct measurements of the elastic constants of the material at room conditions, K' with high-pressure elasticity measurements as well as the bounds provided by thermodynamic identities (Anderson 1995). Such comparisons should always include consideration of the correlation of the parameters from the EoS refinement. Consider, as an example, two independent measurements of K_0 and K' equally offset from the values obtained from the refinement of the 3rd-order BM EoS to the *P-V* data. If only the single-parameter *esd*'s were considered then one would say that measurements represented by points 'A' and 'B' in Figure 4 are both consistent with the *P-V* data, because both lie within the range of the individual error bars. However, when the covariance from the fit of the *P-V* data is considered, it is seen that the values represented by point 'B' lie outside the confidence ellipse for K_0 and K'. Point 'B' is thus inconsistent with the *P-V* data but point 'A', which lies within the confidence ellipse, is consistent.

Independent experimental determinations of K_0 and K' also include both experimental uncertainties and covariance between the parameters that should also be considered. Unfortunately, estimates of the covariances of parameters are rarely available from the literature. For example, the measurement of the elastic constants of quartz by McSkimmin et al. (1965) yielded values of K_{0T} = 37.12(6) GPa and K' = 6.3, for which Levien et al (1980) estimated an uncertainty of +/- 0.3. While the error bars for K_0 and K' overlap with the BM3 fit to the *P-V* compression data (Fig. 5), the point (K_0 = 37.12, K' = 6.3) lies outside the 3σ (99.73%) confidence ellipse for the BM3 fit, and must therefore be said to be inconsistent with this fit to the *P-V* data. If, however, the data of McSkimmin et al. (1965) included a positive correlation of K_0 and K', the confidence ellipse for their results could overlap with that of the BM3 fit. A further worked example of the comparison of datasets from compression measurements and ultrasonic interferometry is provided by Kung et al. (2000).

Evolution of parameter uncertainties. Thus far we have discussed the interpretation and comparison of the EoS parameters at room pressure. But for direct comparison with elasticity data measured at high pressure, for example, it is necessary to obtain the values of the bulk modulus and its pressure derivative(s) at high pressure. The values of these parameters at high pressures follow directly from differentiation of the EoS (Eqns. 1 to 8). The uncertainties in the parameters can then be obtained by transforming the variance-covariance matrix of the least-squares fit of the zero-pressure parameters through Equation (15). This process is mostly clearly illustrated with the Murnaghan EoS because the algebra is simplest. First, expressions for the parameters of interest as a function of the room-pressure parameters and P must be derived. By the definition of the Murnaghan EoS the bulk modulus at pressure P is $K_P = K_0 + PK_0'$, while the high-pressure value of its pressure derivative, K_P', is independent of pressure. Secondly, the derivatives of the high-pressure parameters with respect to those at zero pressure are obtained. For the Murnaghan EoS:

$$\frac{\partial K_P}{\partial K_0} = 1, \quad \frac{\partial K_P}{\partial K_0'} = P, \quad \frac{\partial K_P'}{\partial K_0} = 0, \quad \frac{\partial K_P'}{\partial K_0'} = 1 \tag{25}$$

The elements of the variance-covariance matrix at a pressure P, $\mathbf{V}^{\mathbf{P}}$, is then obtained in terms of the variance-covariance matrix, $\mathbf{V}^{\mathbf{0}}$, of the refined zero-pressure parameters by substituting these derivatives into Equation (15), thus:

$$\begin{aligned}
\mathbf{V}^{\mathbf{P}}_{\mathbf{K,K}} &= \mathbf{V}^{\mathbf{0}}_{\mathbf{K,K}} + 2P\mathbf{V}^{\mathbf{0}}_{\mathbf{K,K'}} + P^2\mathbf{V}^{\mathbf{0}}_{\mathbf{K',K'}} \\
\mathbf{V}^{\mathbf{P}}_{\mathbf{K',K'}} &= \mathbf{V}^{\mathbf{0}}_{\mathbf{K',K'}} \\
\mathbf{V}^{\mathbf{P}}_{\mathbf{K,K'}} &= \mathbf{V}^{\mathbf{0}}_{\mathbf{K,K'}} + P\mathbf{V}^{\mathbf{0}}_{\mathbf{K',K'}}
\end{aligned} \tag{26}$$

The uncertainties in K_P and K_P' are then $\sqrt{\mathbf{V}^{\mathbf{P}}_{\mathbf{K,K}}}$ and $\sqrt{\mathbf{V}^{\mathbf{P}}_{\mathbf{K',K'}}}$ respectively. The second of the expressions in Equation (26) shows that the uncertainty in K_P' is independent of pressure, which is only true for the Murnaghan EoS. Other EoS display a small variation in this uncertainty with pressure (e.g. Bell et al. 1987). The last expression in Equation (26) indicates that the covariance of K_P and K_P' becomes zero at a pressure $P_{\min} = -\mathbf{V}^{\mathbf{0}}_{\mathbf{K,K'}} / \mathbf{V}^{\mathbf{0}}_{\mathbf{K',K'}}$. At this pressure the values of K_P and K_P' are determined completely independently of one another and the uncertainty in the bulk modulus is at a minimum value (Fig. 6). The evolution of the variance-covariance matrix with pressure (Eqn. 26) results in a rotation of the confidence ellipse for K_P and K_P' as pressure is increased (Fig. 7). Note especially that at pressures above P_{min}, K_P and K_P' are *positively* correlated.

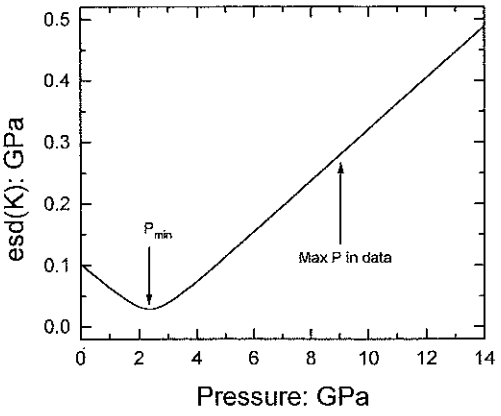

Figure 6. The variation with pressure of the uncertainty of the bulk modulus for a Murnaghan EoS fitted to the quartz *P-V* data (Table 1), calculated with Equation (26).

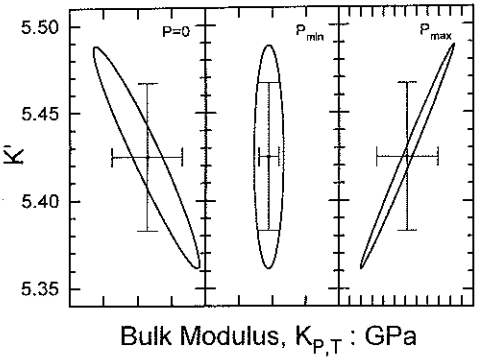

Figure 7. The evolution of the 68.3% confidence ellipse for K_0 and K' for a Murnaghan EoS fitted to the quartz *P-V* data (Table 1), calculated with Equation (26). Each tick mark on the horizontal axis is 0.1 GPa. At P_{min} the covariance is zero, and at higher pressures K_0 and K' are positively correlated.

If the *P-V* data are separated by approximately equal intervals in pressure, then P_{min} is between 25% and 50% of the maximum pressure in the data set. Similar conclusions were obtained by Bell et al. (1987) through numerical simulations of *P-V* data. The exact value of P_{min} depends on the exact distribution of the data and the relative uncertainties of the data points (see Kung et al. 2000 for another example). Nonetheless, Figure 6 demonstrates the general truth that EoS parameters are best constrained at pressures towards the middle of the data set, and that the uncertainties increase rapidly outside the pressure range over which the *P-V* data were measured.

Choice of EoS formalism. Schlosser and Ferrante (1988) showed that the Vinet and the Birch-Murnaghan EoS are algebraically equivalent to low orders in compression, and thus provide equally good descriptions of the volume variation with pressure for "small" compressions. The value of compression at which the two EoS diverge significantly is dependent upon the value of K'. For $K' < 3.3$ and $K' > 7$ the BM3 EoS yields lower pressures than the Vinet for a given compression or, equivalently, lower volumes (larger η) for a given pressure (Fig. 8a). For $3.3 < K' < 7$ the opposite is true, with the BM3 EoS yielding pressures that are 1.2% higher than the Vinet EoS at $\eta = 0.80$ for $K' = 4$. For values of $K' \sim 3.3$ and 7 there is no significant divergence to much larger values of compression (Fig. 8a). The practical result is that within these bounds, fits of the Vinet and the Birch-Murnaghan 3rd-order EoS to *P-V* data yield indistinguishable values for K_0 and K' (Table 1, also Schlosser and Ferrante 1988, Jeanloz 1988). Therefore the choice between these two EoS is not significant for compression to $\eta \sim 0.85$, and values of K_0 and K' from a fit in one EoS can be used in the other EoS formalism.

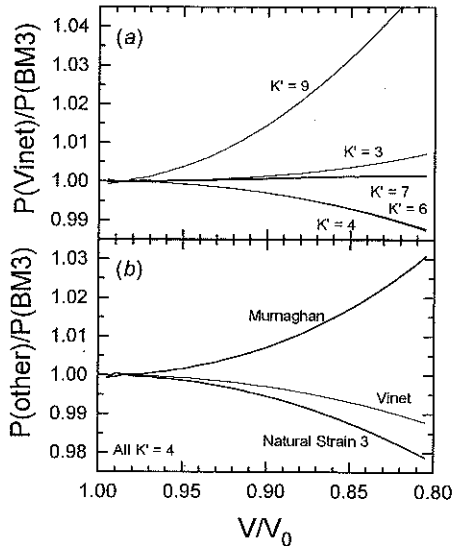

Figure 8. Comparison of the pressures predicted by different EoS as a function of compression. (a) The ratio of pressure from the Vinet EoS to that from the Birch-Murnaghan 3rd order EoS for various K' (after Jeanloz 1988). (b) A comparison of other EoS for $K'=4$.

By contrast the divergence of both the Murnaghan and the 3rd-order Natural Strain EoS from the BM3 occurs at smaller compressions (Fig. 8b) and the divergence increases with increasing K'. For the Murnaghan the positive deviation in Figure 8b arises from the implied value of K'' being zero. In the 3rd-order Natural Strain EoS (Eqn. 5) the implied value of K'' is much larger than that of either the Vinet or the BM3 EoS (Eqns. 4 and 8) which are very similar to one another (e.g. Table 1), and the deviation is therefore negative. The implications for fitting *P-V* data with these two EoS is that they provide a significantly poorer fit to the data, as well as refined values of K_0 and K' that differ significantly from the values derived from fits of either the Vinet or the BM3 EoS (e.g Table 1). It is also found that the value of K_0 obtained from the latter is in much better agreement with independent determinations, for example from measurements of the elasticity (e.g. Angel et al. 1997). While the fit of the Natural Strain EoS can be improved by extension to the 4th-order, there is no remedy for the mis-fit of the Murnaghan EoS which should therefore not be used to fit *P-V* data to more than ~10% compression. Similarly, the divergence of these two EoS from the Vinet and the BM3 means that EoS parameters should not be transferred to or from the Natural Strain or the Murnaghan EoS (Fig. 1).

PREDICTION OF UNCERTAINTIES

Theory

It is clear from the formulation of all EoS (Eqns. 1-8) that an improvement in the precision of P,V data by either a reduction in σ_P or σ_v will lead to a more precise determination of the bulk modulus and K'. Similarly, because of the non-dimensional form of all EoS, it is also clear that reduction in the uncertainties of K_0 and K' can also be achieved by either increasing the number of data points or by increasing the pressure range of the measurements while maintaining the precision of the individual measurements. However, the relationship between the final uncertainties in K_0 and K' and the experimental parameters of measurement precision (i.e. σ_P and σ_v), number of data, and pressure range is not straightforward. Bass et al (1981) therefore developed an algorithm (extended by Liebermann and Remsberg 1986) that predicts the values of σ_K and $\sigma_{K'}$ expected from a

given set of these experimental parameters, at least for isothermal datasets. The algorithm is based upon a linearization of the BM3 EoS, and its fitting by the method of linear least-squares. The method is presented here in a little more detail, together with a few extensions based on the work of Liebermann and Remsberg (1986) and some corrections to typographical errors that occur in the appendix of the original paper.

The BM3 EoS (Eqn. 3) can be written as a linear combination of functions of compression η:

$$P = a_1 f_1(\eta) + a_2 f_2(\eta) \tag{27}$$

where $f_1(\eta) = (\eta^{-7/3} - \eta^{-5/3})$ and $f_2(\eta) = f_1(\eta)(\eta^{-2/3} - 1)$ and the two coefficients are:

$$a_1 = \frac{3}{2} K_0 \qquad a_2 = \frac{3}{4} a_1 (K' - 4) \tag{28}$$

Equation (27) can then be written in matrix form as $\boldsymbol{P} = \boldsymbol{AF}$ for the whole P,V dataset. Here, $\boldsymbol{P}$ is a vector of i components, each of which is the pressure of a volume datum. $\boldsymbol{F}$ is a matrix, the i'th line of which contains the functions $f_1(V_i)$ and $f_2(V_i)$ of the volume V_i at each pressure P_i, and $\boldsymbol{A}$ is a column vector of the two coefficients a_1 and a_2 that are to be determined. Note that in this formulation, as in the f-F plot, the value of V_0 is assumed to be known exactly. This is not correct but, as will be demonstrated, reasonable estimates of the parameter uncertainties are still obtained. The formulation of the BM3 EoS given in Equation (27) is *linear* in the parameters a_1 and a_2, so the least-squares solution for the vector of coefficients $\boldsymbol{A}$ is then given directly (without need for iteration) by

$$\mathbf{A} = \left(\mathbf{F}^{\mathrm{T}}\mathbf{W}\mathbf{F}\right)^{-1}\mathbf{F}^{\mathrm{T}}\mathbf{W}\mathbf{P} \tag{29}$$

where $\boldsymbol{W}$ is the weighting matrix, defined as before: its diagonal terms are σ_i^{-2} and its off-diagonal terms are zero. The variance-covariance matrix for the refined values of the parameters a_1 and a_2 is then

$$\boldsymbol{V} = (\boldsymbol{F}^{\mathrm{T}}\boldsymbol{W}\boldsymbol{F})^{-1} \tag{30}$$

The variance-covariance matrix for K_0 and K' is obtained by transforming $\boldsymbol{V}$ according to Equation (15). The differentials of the K_0 and K' required for the transformation are, from Equation (28):

$$\frac{\partial K_0}{\partial a_1} = \frac{2}{3}, \qquad \frac{\partial K_0}{\partial a_2} = 0, \qquad \frac{\partial K'}{\partial a_1} = \frac{-4a_2}{3a_1^2}, \qquad \frac{\partial K'}{\partial a_2} = \frac{4}{3a_1} \tag{31}$$

and the elements of the variance-covariance matrix for K_0 and K' are then:

$$\begin{aligned} V_{K,K} &= 2V_{1,1}/3 \\ V_{K',K'} &= V_{11}\left(\frac{4a_2}{3a_1^2}\right)^2 - V_{12}\left(\frac{4a_2}{3a_1^2}\right)\left(\frac{4}{3a_1}\right) + V_{22}\left(\frac{4}{3a_1}\right)^2 \\ V_{K,K'} &= \frac{2}{3}\left[V_{12}\left(\frac{4}{3a_1}\right) - V_{11}\left(\frac{4a_2}{3a_1^2}\right)\right] \end{aligned} \tag{32}$$

The extension of this approach to the BM4 equation of state, or its adaptation to the Natural Strain or the Vinet EoS in their linear forms is straight-forward, but is not necessary for compressions up to ~15% because these EoS result in similar esd's in the fitted parameters in this regime (e.g. Table 1). Thus the calculation based upon the BM3

EoS can be used as a useful proxy for these other EoS. The extension of this analysis to *P-V-T* data is however non-trivial, because the thermal expansion coefficient (Eqn. 9) appears within the functions f_1 and f_2 as part of η.

The practical process of uncertainty estimation proceeds by calculating a set of synthetic *P-V* data from an estimate of the EoS parameters V_0, K_0 and K'. This synthetic data-set is used to construct the matrix $\boldsymbol{F}$. Probable uncertainties in σ_V and σ_P are also assigned to each data point, and the total uncertainty σ_i for each data point then follows from Equation (13); this differs from the method of Bass et al. (1981) in that they used K_0, instead of the value of K, at each pressure datum to convert the σ_V to σ_P through Equation (13). The nett result is that the uncertainties calculated here are of the order of 20% higher than those calculated by Bass et al. (1981), and the variation with the number of data in a data set is slightly different. The diagonal elements of $\boldsymbol{W}$ are then set equal to σ_i^{-2} as usual, and the calculation of the expected uncertainties follows directly from application of Equations (30) and (32).

Although any synthetic data-set can be modelled in this way, it is useful to make some further assumptions in order to automate the process. In the following calculations it will be assumed that the data are equally spaced in pressure and that the absolute uncertainties in both pressure and volume are constant over the data-set. Note that this means that the uncertainty in compression increases with increasing pressure because as V becomes smaller, σ_V/V becomes larger, while the fractional uncertainty in pressure decreases. With these assumptions the agreement between the uncertainties predicted for K_0 and K' with those obtained from fitting experimental data is reasonable (e.g. Fig. 9). Note that the calculation does not account for intrinsic uncertainties in the pressure scale itself which, if accounted for, will increase the uncertainties of both K_0 and K'.

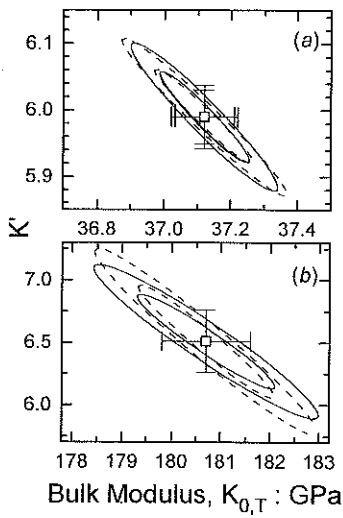

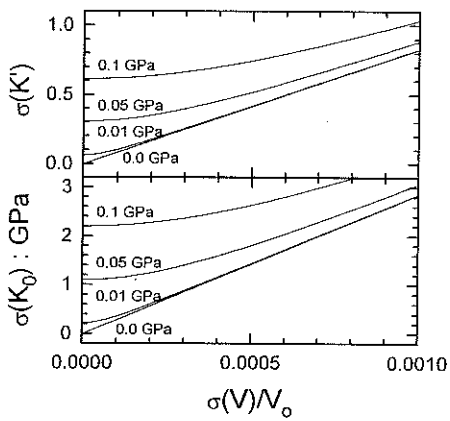

Figure 9 (left). Comparison of predicted (dashed lines) confidence ellipses with those obtained by least-squares fitting of experimental data. (a) Quartz *P-V* data from Angel et al. (1997). (b) *P-V* data for braunite from Miletich et al. (1998). In both cases the experimental values for n, K_0 and K' and the average experimental values for σ_V/V_0, and σ_P were used in the calculation of the predicted variance-covariance matrix through Equations (30)-(32).

Figure 10 (right). Predicted uncertainties in K' and K_0 as a function of σ_V/V_0 for a data-set of 10 *P-V* data from a material with $K_0 = 100$ GPa and $K' = 4$, measured to a maximum pressure of 10 GPa. Numbers on the plots are σ_P.

General results

The general form of the variation of σ_K and $\sigma_{K'}$ with the precision in volume measurement is shown in Figure 10 (above) for a material with K_0 = 100 GPa, K' = 4, measured at 10 equally spaced pressure points up to a maximum of 10 GPa. For σ_v/V_0 = 0.0 the data point uncertainties become (Eqn. 13) equal to σ_P alone. Then all of the elements of V will scale with σ_P (Eqn. 30), and the uncertainties in both K_0 and K' scale exactly with the uncertainties in pressure. For small uncertainties the volume, essentially up to $\sigma_v/V_0 < \sigma_P/K_0$ (from Eqn. 13), the final uncertainties in both EoS parameters remain dominated by the uncertainty in pressure. Modern single-crystal X-ray diffraction experiments (σ_P = 0.01 GPa, $\sigma_v/V_0 = 10^{-4}$; Angel et al., this volume) fall in this regime for most crustal minerals (K_0 <100 GPa). At these levels, halving σ_P halves σ_K while reducing σ_v will have very little influence on the final results. However, because σ_K is already so small, this reduction amounts to only a 0.1 GPa improvement in the precision of K_0. Thus one would conclude that no further useful improvement in precision could be obtained for an experiment represented by these parameters.

By contrast, for $\sigma_v/V_0 > 2\sigma_P/K_0$ (Liebermann and Remsberg 1986) the uncertainty in the volume measurements dominates the experimental constraints on K_0 and K', and the curves lie sub-parallel to that for zero pressure uncertainty (Fig. 10). Thus, if data are measured with σ_v/V_0=0.001 (=1 part in 1,000) and σ_P =0.05 GPa then reducing the pressure measurement uncertainty will only reduce σ_K at most by 0.2 GPa (Fig. 10b), whereas improving the precision of the volume measurement by a factor of 2 will halve the values of σ_K and $\sigma_{K'}$. If pressure is being measured by an internal diffraction standard (e.g. Miletich et al. this volume) then an added bonus will be a reduction in pressure uncertainty by a factor of 2, and a further reduction in the final uncertainties.

For softer materials measured over the same pressure range there will be a larger amount of total compression, so the precision in the determined values of K_0 and K' will be improved. For σ_v/V_0 =0 this improvement scales exactly as the bulk modulus, provided K' remains constant (Fig. 11), and approximately as the bulk modulus for $\sigma_v/V_0 < \sigma_P/K_0$. This follows because the total compression scales approximately as P_{max}/K_0. But at larger values of σ_v/V_0 the scaling law does not hold because of the form of Equation (13); an experiment on the material that is more compressible by a factor of 2 yields uncertainties about 1/3 those obtained from the harder material. If the pressure derivative of the bulk modulus is higher, then the total compression achieved over a given pressure range is reduced and the precision in the EoS parameters is consequently reduced. The actual scaling law at low σ_v/V_0 is related to the average value of K over the pressure range, but note that the effect of different K' values on the esd(K) is small.

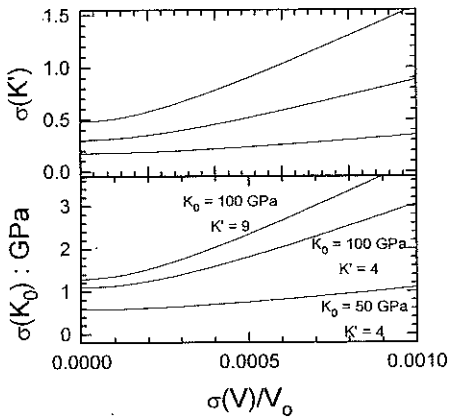

Figure 11. Predicted uncertainties in K' and K_0 as a function of σ_V/V_0 for datasets of 10 P-V data from materials with different K_0 and K', measured to a maximum pressure of 10 GPa, with σ_P = 0.05 GPa.

If improvements in the precision of individual measurements do not yield significant improvements in the precision of K_0 and K', then increasing the

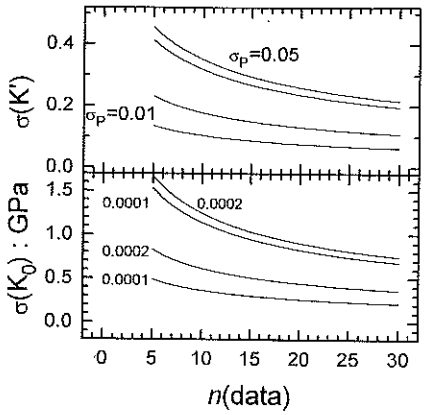

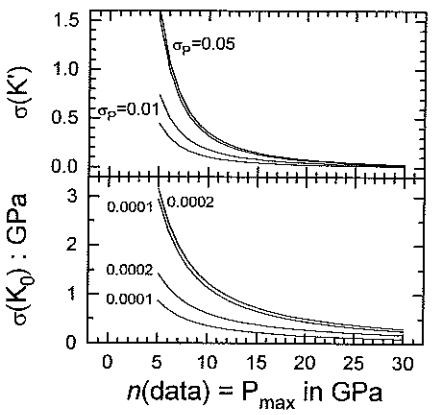

Figure 12 (left). Predicted uncertainties in K' and K_0 as a function of the number of equally-spaced *P-V* data from a material with K_0 = 100 GPa, K' = 4 and two values of σ_P, measured to a maximum pressure of 10 GPa. Values of σ_V/V_0 are given on the lower plot.

Figure 13 (right). Predicted uncertainties in K' and K_0 as a function of the number of *P-V* data, at a fixed interval of 1 GPa from a material with K_0 = 100 GPa, K' = 4 and two values of σ_P. Values of σ_V/V_0 are given on the lower plot. The maximum pressure of each experiment in GPa is equal to the number of data points.

number of measured data may do so. This may be achieved in two ways. Figure 12 shows the effect of increasing the number of data, n, measured over the same pressure interval (10 GPa). As the number of data are first increased the uncertainties in the refined parameters decrease sharply, approximately proportional to $n^{1/2}$, as expected. But for higher values of n the uncertainties asymptote to a finite value dependent on σ_v and σ_P. Figure 12 shows that for σ_P =0.01 GPa, there is very little to be gained by collecting more than 10 data, while for experiments with σ_P =0.05 GPa significant improvements can still be made by collecting up to 20 data. The gain in precision is greater if the pressure range over which the data-set is collected is increased while maintaining the pressure interval of the data constant at 1.0 GPa (Fig. 13). Here the scaling law is stronger than $n^{1/2}$ (actually about $n^{3/2}$) for $n < 20$ as a result of the increased maximum compression (contributing $\sim n$) and the increased number of data (contributing $\sim n^{1/2}$). In considering the results of these calculations it must be remembered that they are only intended to act as a guide for elements of experimental design, such as the number of data points to be collected. It must also be remembered that the calculations can only reflect the results of experimental precision or reproducibility and do not include the influence of systematic errors such as inaccuracy in experimental pressure scales or the presence of non-hydrostatic stresses.

ACKNOWLEDGMENTS

I thank Nancy Ross, Steve Jacobsen, Jennifer Kung and Ronald Miletich for various collaborations, and their testing of various computer programs, all of which contributed to this chapter. In addition, Bob Hazen, Alex Pavese, and Alan Woodland provided many helpful comments and suggestions for improvement of the original manuscript. Bob Liebermann kindly provided an unpublished manuscript that provided the basis for the last section of this chapter, and Jean-Paul Poirier patiently answered my questions about the Natural Strain EoS.

APPENDIX

The computer program EOSFIT, written by the author, fits all of the EoS described in this chapter to *P-V* and *P-V-T* data, as well as performing fits of cell parameter variations with *P* and *T*, by the method of non-linear least-squares. Refinements can be run with a choice of weighting schemes and the parameters to be refined. All statistical measures described in this chapter are provided as output. EOSFIT, along with a number of subsidary programs to perform the associated calculations described in this chapter, and the STRAIN program of Ohashi (1972) are available by e-mail from the author.

REFERENCES

Anderson OL (1995) Equations of state of solids for geophysics and ceramic science. Oxford University Press, Oxford, UK

Angel RJ, Allan DR, Miletich R, Finger LW (1997) The use of quartz as an internal pressure standard in high-pressure crystallography. J Appl Crystallogr 30:461-466

Bass JD, Liebermann RC, Weidner DJ, Finch SJ (1981) Elastic properties from acoustic and volume compresssion experiments. Phys Earth Planet Int 25:140-158

Bell PM, Mao HK, Xu JA (1987) Error analysis of parameter-fitting in equations of state for mantle minerals. *In* Manghnani MH and Syono Y (eds) High-pressure Research in Mineral Physics, p 447-454. Terra Scientific Publishing Co, Tokyo

Birch F (1947) Finite elastic strain of cubic crystals. Phys Rev 71:809-824

Chatterjee ND, Krüger R, Haller G, Olbricht W (1998) The Bayesian approach to an internally consistent thermodynamic database: theory, database, and generation of phase diagrams. Contrib Mineral Petrol 133:149-168

Duffy TS, Wang Y (1998) Pressure-volume-temperature equations of state. *In* Hemley RJ (ed) Ultra-High-Pressure Mineralogy. Rev Mineral 33:425-457

Fei Y (1995) Thermal expansion. *In* Ahrens TJ (ed) Mineral Physics and Crystallography, A Handbook of Physical Constants. Am Geophys Union, Washington, DC

Hazen RM, Finger LW (1989) High-pressure crystal chemistry of andradite and pyrope: revised procedures for high-pressure diffraction experiments. Am Mineral 74:352-359

Heinz DL, Jeanloz R (1984) The equation of state of the gold calibration standard. J Appl Phys 55:885-893

Hofmeister AM (1993) Interatomic potentials calculated from equations of state: limitation of finite strain to moderate K'. Geophys Res Letts 20:635-638

Holland TJB, Powell R (1998) An internally consistent thermodynamic data set for phases of petrological interest. J Metamorph Geol 16:309-343

Jeanloz R (1981) Finite strain equation of state for high-pressure phases. Geophys Res Letts 8:1219-1222.

Jeanloz R (1988) Universal equation of state. Phys Rev B 38:805-807

Jessen SM, Küppers H (1991) The precision of thermal-expansion tensors of triclinic and monoclinic crystals. J Appl Crystallogr 24:239-242

Krishnan RS, Srinavasan R, Devanarayanan S (1979) Thermal Expansion of Crystals. Pergamon Press, Oxford

Kung J, Angel RJ, Ross NL (2000) Elasticity of $CaSnO_3$ perovskite. Phys Chem Minerals (submitted)

Levien L, Prewitt CT, Weidner DJ (1980) Structure and elastic properties of quartz at pressure. Am Mineral 65:920-930

Liebermann RJ, Remsberg AR (1986) Elastic behaviour of minerals from acoustic and static compression studies. US-Japan Seminar on High-Pressure Research. Applications in Geophysics and Geochemistry, Program with Abstracts, 84-85

Lybanon M (1984) A better least-squares method when both variables have uncertainties. Am J Phys 52:22-26

McSkimmin HJ, Andreatch P, Thurston RN (1965) Elastic moduli of quartz versus hydrostatic pressure at 25° and -195.8°C. J Appl Phys 36:1624-1633

Miletich RM, Allan DR, Angel RJ (1998) Structural control of polyhedral compression in synthetic braunite, $Mn^{2+}Mn^{3+}{}_6O_8SiO_4$. Phys Chem Minerals 25:183-192

Murnaghan FD (1937) Finite deformations of an elastic solid. Am J Math 49:235-260

Nye JF (1957) Physical Properties of Crystals. Oxford University Press, Oxford

Ohashi (1972) Program Strain. Program lisiting provided in Hazen and Finger (1982) Comparative Crystal Chemistry, John Wiley and Sons, New York.

Orear J (1982) Least-squares when both variables have uncertainties. Am J Phys 50:912-916

Paufler PP, Weber T (1999) On the determination of linear thermal expansion coefficients of triclinic

crystals using X-ray diffraction. Eur J Mineral 11:721-730
Plymate TG, Stout JH (1989) A five-parameter temperature-corrected Murnaghan equation for P-V-T surfaces. J Geophys Res 94:9477-9483
Poirier J-P, Tarantola A (1998) A logarithmic equation of state. Phys Earth Planet Int 109:1-8
Press WH, Flannery BP, Teukolsky SA, Vetterling WT (1986) Numerical Recipes—The Art of Scientific Computing. Cambridge University Press, Cambridge.
Prince E, Boggs PT (1992) Refinement of structural parameters, 8.1: Least-squares. *In* AJC Wilson (ed) International Tables for X-ray Crystallography, Vol. C. Int'l Union of Crystallography, Kluwer Academic Publishers, Dordrecht, The Netherlands
Prince E, Spiegelman CH (1992a) Refinement of structural parameters, 8.4: Statistical significance tests. In AJC Wilson (ed) International Tables for X-ray Crystallography, Vol. C. Int'l Union of Crystallography, Kluwer Academic Publishers, Dordrecht, The Netherlands
Prince E, Spiegelman CH (1992b) Refinement of structural parameters, 8.5: Detection and treatment of systematic error. *In* AJC Wilson (ed) International Tables for X-ray Crystallography, Vol. C. Int'l Union of Crystallography, Kluwer Academic Publishers, Dordrecht, The Netherlands
Reed BC (1992) Linear least-squares fits with errors in both coordinates. II: Comments on parameter variances. Am J Phys 60:59-62
Saxena SK, Zhang J (1990) Thermochemical and pressure-volume-temperature systematics of data on solids, Examples: Tungsten and MgO. Phys Chem Minerals 17:45-51
Schlenker JL, Gibbs GV, Boisen MB (1975) Thermal expansion coefficients for monoclinic crystals: a phenomenological approach. Am Mineral 60:828-833
Schlosser H, Ferrante J (1988) Universality relationships in condensed matter: Bulk modulus and sound velocity. Phys Rev B 37:4351-4357
Stacey FD, Brennan BJ, Irvine RD (1981) Finite strain theories and comparisons with seismological data. Geophys Surveys 4:189-232
Vinet P, Ferrante J, Smith JR, Rose JH (1986) A universal equation of state for solids. J Phys C: Solid State 19:L467-L473
Vinet P, Ferrante J, Rose JH, Smith JR (1987a) Compressibility of solids. J. Geophys Res 92:9319-9325
Vinet P, Smith JR, Ferrante J, Rose JH (1987b) Temperature effects on the universal equation of state of solids. Phys Rev B 35:1945-1953
Young RA (1995) The Rietveld Method. Int'l Union of Crystallography, Oxford University Press, Oxford.
Zhao Y, Schiferl D, Shankland TJ (1995) A high P-T single-crystal X-ray diffraction study of thermoelasticity of $MgSiO_3$ orthoenstatite. Phys Chem Minerals 22:393-398